Dentomaxillofacial Radiology (2016) 45, 20150302
© 2015 The Authors. Published by the British Institute of Radiology
birpublications.org/dmfr

RESEARCH ARTICLE

A comparative study of new and current methods for dental micro-CT image denoising

[1]Mahdi Shahmoradi, [2]Mojtaba Lashgari, [2,3]Hossein Rabbani, [4]Jie Qin and [1,5]Michael Swain

[1]Biomaterials and Bioengineering, Faculty of Dentistry, University of Sydney, Sydney, Australia; [2]Department of Biomedical Engineering, Faculty of Advanced Medical Technology, Isfahan University of Medical Sciences, Isfahan, Iran; [3]Medical Image & Signal Processing Research Center, Isfahan University of Medical Sciences, Isfahan, Iran; [4]Department of Implantology, Stomatological Hospital, Jilin University, Changchun, Jilin, China; [5]Department of Bio-clinical Sciences, Faculty of Dentistry, Health Sciences Centre, Kuwait University, Kuwait

Objectives: The aim of the current study was to evaluate the application of two advanced noise-reduction algorithms for dental micro-CT images and to implement a comparative analysis of the performance of new and current denoising algorithms.
Methods: Denoising was performed using gaussian and median filters as the current filtering approaches and the block-matching and three-dimensional (BM3D) method and total variation method as the proposed new filtering techniques. The performance of the denoising methods was evaluated quantitatively using contrast-to-noise ratio (CNR), edge preserving index (EPI) and blurring indexes, as well as qualitatively using the double-stimulus continuous quality scale procedure.
Results: The BM3D method had the best performance with regard to preservation of fine textural features (CNR_{Edge}), non-blurring of the whole image (blurring index), the clinical visual score in images with very fine features and the overall visual score for all types of images. On the other hand, the total variation method provided the best results with regard to smoothing of images in texture-free areas ($CNR_{Tex\text{-}free}$) and in preserving the edges and borders of image features (EPI).
Conclusions: The BM3D method is the most reliable technique for denoising dental micro-CT images with very fine textural details, such as shallow enamel lesions, in which the preservation of the texture and fine features is of the greatest importance. On the other hand, the total variation method is the technique of choice for denoising images without very fine textural details in which the clinician or researcher is interested mainly in anatomical features and structural measurements.
Dentomaxillofacial Radiology (2016) **45**, 20150302. doi: 10.1259/dmfr.20150302

Cite this article as: Shahmoradi M, Lashgari M, Rabbani H, Qin J, Swain M. A comparative study of new and current methods for dental micro-CT image denoising. *Dentomaxillofac Radiol* 2016; **45**: 20150302.

Keywords: noise; dental; X-ray microtomography; image quality enhancement; computer-assisted image processing

Introduction

Micro CT (micro-CT) is an X-ray attenuation method for the study of the internal structure of materials and hard biological tissues with a high resolution and in three dimensions.[1] In recent years, micro-CT has been widely utilized in dentistry for the assessment of mineral density distribution patterns of the bone and dental tissues and of the microstructure of dental biomaterials.[2] Despite various advantages of micro-CT, the produced images can suffer from a range of artefacts such as image noise, beam hardening and ring

Correspondence to: Dr Hossein Rabbani. E-mail: h_rabbani@med.mui.ac.ir
The first author thanks the Australian Dental Research Foundation (ADRF) for ADRF grants (84-2012 and 71-2013) and the University of Sydney for USydIS Scholarship.
Received 16 September 2015; revised 8 January 2016; accepted 12 January 2016

artefact, all of which affect the diagnostic quality of the images.[3,4]

Image noise is a particularly important artefact in micro-CT imaging which reduces the contrast resolution and degrades the image quality. The noise content also prevents the effective performance of image processing and analysis algorithms such as edge detection, feature segmentation and three-dimensional (3D) volume rendering which are very sensitive to noise. Furthermore, low noise and unblurred images are essential for many studies such as cariology and associated remineralization research where reliable detection and quantification of the demineralized area require clear images with definable borders.[5]

Noise removal for biomedical images is a vital and challenging task as it requires the elimination of extraneous and spurious signals while preserving the fine details pertaining to the diagnostic information. Generally, denoising algorithms use a generic local or global image as the smoothness model which is desired following noise minimization.[6] Although various denoising approaches have been developed and tested for different types of medical images,[7] only a few basic methods such as the gaussian[8–11] and median[12,13] filtering methods have been applied for denoising dental micro-CT and other types of maxillofacial images.

Considering the significant increase in the application of CT systems in clinical dentistry[14] and maxillofacial research,[2] there is a great need for efficient and robust methods for denoising dental radiographs. Therefore, the aim of the current study is to evaluate the application of two advanced noise reduction algorithms for dental micro-CT images and to implement a comparative analysis of the performance of new and current denoising algorithms.

Methods and materials

Tooth samples

Extracted teeth were collected from the oral surgery department at the Sydney Dental Hospital, University of Sydney, NSW, Australia, according to protocols approved by the Sydney Local Health District ethics committee, protocol X12-0065 and HREC/12/RPAH/106.

Data acquisition and image reconstructing

Imaging was performed using a high-resolution micro-CT system (Skyscan 1172; Skyscan, Aartsellar, Belgium). Imaging was undertaken using continuous mode exposures at 0.5-s intervals and a binning value of 2, with an accelerating voltage of 60 kV and a current of 120 μA. The samples were rotated over 360° at 0.14° rotation steps producing 2571 projections. The resultant reconstructed images had an isotropic pixel resolution of 8.9 μm and a dynamic range of 16 bits with an image matrix of 1000 × 1000 pixels.

Image denoising

Compilation of the algorithms and quantitative analysis of the proposed denoising methods were implemented using MATLAB® v. 7.11.0.584 (R2010b) (MathWorks® Inc., Natick, MA) on a computer system with Intel® Core™ i7 central processing unit (Q740 @1.73 GHz) and 4.00-GB random-access memory (Intel Corporation, Santa Clara, CA).

Transverse micro radiography (TMR) images of thin sections of the teeth[15] were considered as the generic smoothness model. Considering the TMR images and assuming the homogeneous structure of the enamel and dentin which is mainly composed of uniform hydroxyapatite

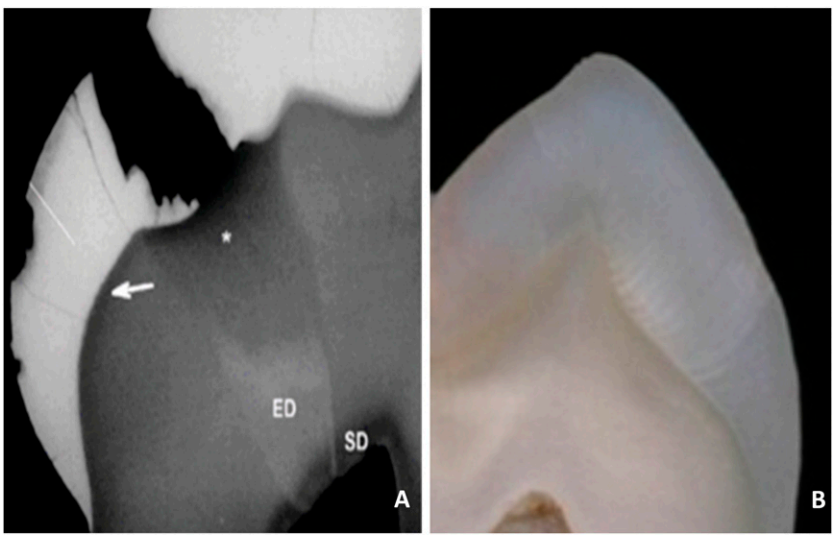

Figure 1 (a) Transverse micro radiography image of a thin section of a tooth with a cavitated lesion. Reproduced from De Medeiros et al[15] with permission from John Wiley and Sons. (b) Optical image of a ground section of a premolar tooth.

crystals,[16] the noise-free images were expected to have a smooth and non-textural appearance (Figure 1).

Following tomographic reconstruction, sectional images were selected randomly from the associated image stack of each specimen and were consequently imported into MATLAB. Denoising of the images was performed using gaussian and median filters as current approaches, and the block-matching and 3D (BM3D)[17,18] and total variation[19] methods as the proposed new filtering methods.

Gaussian filters are a class of linear filters with the weight chosen based on the shape of a gaussian function (normal distribution). In this filter, two initial arbitrary parameters, *i.e.* radius and standard deviation, are used to create a two-dimensional matrix with gaussian distribution which is used to convolve the image. The transformation, which is calculated using the gaussian function, is applied to each pixel of the image.

Median filters are among the class of non-linear image-smoothing filters which use the median of the neighbourhood of the pixel in the original image. With this filter, all pixels of the neighbourhood, which are identified by a mask (window), are sorted in order (*i.e.* the gray level), and the median value is calculated and set as the pixel value. Following the application of this filter, the pixel values which are very different from the neighbouring pixels are eliminated, and the median value of pixels within the defined mask is assigned instead. The arbitrary length of the mask is determined by the user.[20]

The total variation denoising or regularization method is based on the principle that images with

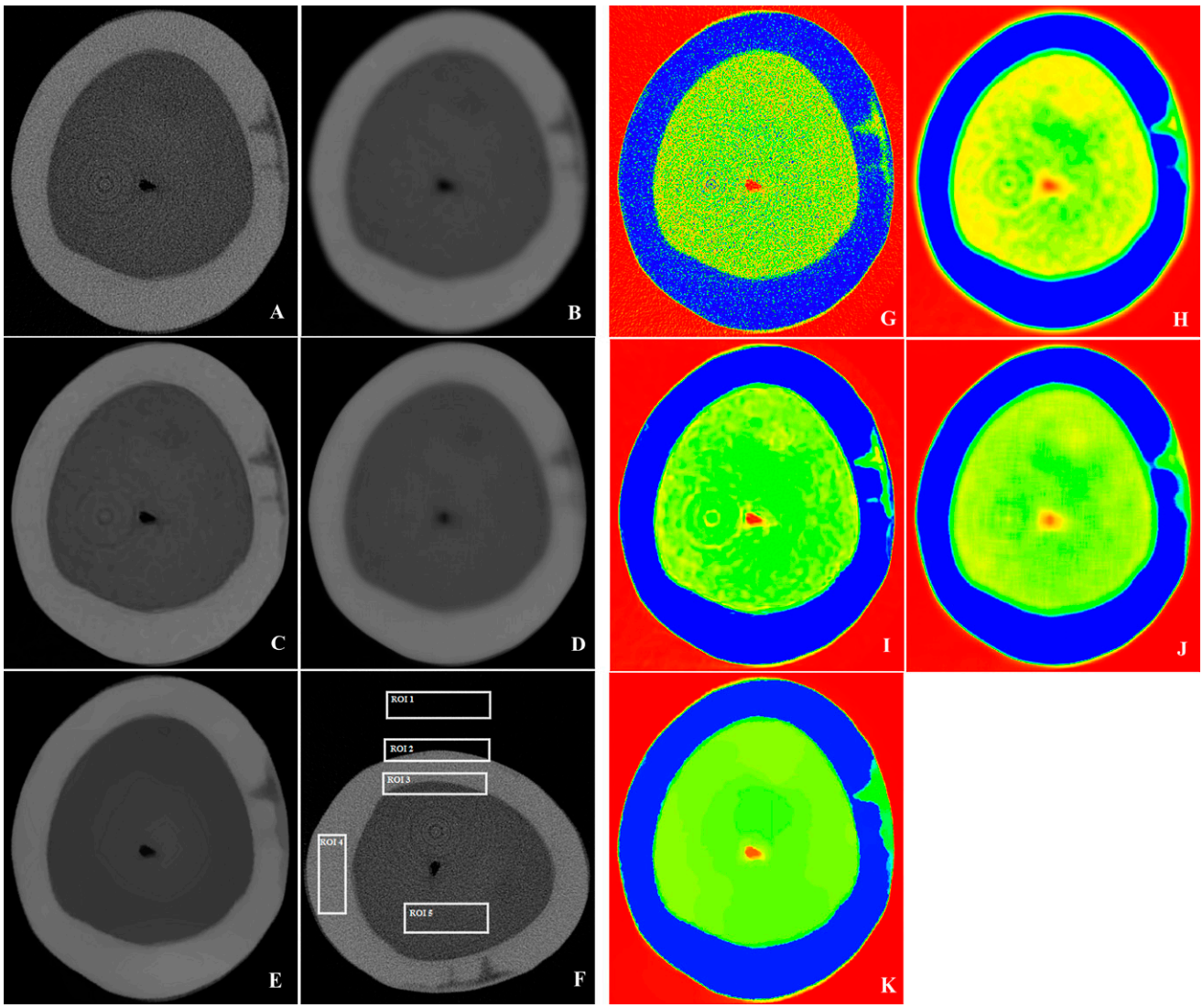

Figure 2 Observations of an individual slice of a tooth with proximal enamel caries before and following processing using various filter options and colourization: (a, g) original image; (b, h) gaussian blur filtering; (c, i) block-matching and three-dimensional filtering; (d, j) median filtering; (e, k) total variation filtering; (f) regions of interest (ROIs).

excessive details have high total variation.[21] One of the consequences of the presence of noise in images is the increase in the variation of pixel values among adjacent pixels. In noise-free images, such amount of variation in the value of the neighbouring pixels usually exists mainly at the edges, and the extent of the variation in smooth and texture-free areas is lower than in noisy images, which have a greater amount of total variation. According to the above-mentioned principle, reducing the total variation of the signal, subject to it being a close match to the original signal, eliminates the undesired details whilst preserving important information such as edges. The main advantage of this technique is the simultaneous preservation of edges whilst smoothing the noise in homogeneous regions.[19]

BM3D denoising, proposed by Dabov et al,[18] is a state-of-the-art denoising method which is based on sophisticated mathematical theories and framework. Simply speaking, the algorithm performs the denoising in three steps:[17]

(1) *Analysis*: similar patches from the image are recognized and collected in groups. Each group forms a 3D stack using an invertible 3D transform, which enables relocation of each patch of each stack to its original place in the image.
(2) *Processing*: the 3D stacks are filtered by a hard-thresholding denoising method based on wavelet transform.
(3) *Synthesis*: the filtered stacks, which are actually filtered patches, provide an initial estimation of the denoised image for each patch. The filtered patches are relocated to form the new image. The final denoised image is calculated as a weighted average of all the filtered patches.

Quantitative analysis of denoising methods

The performance of the above-mentioned denoising methods was evaluated quantitatively using the following three image analysis parameters:

Contrast-to-noise ratio

The contrast-to-noise ratio (CNR) is a physical index, which is intended to simulate human image perception. Basically, the CNR is the measurement of the contrast between a feature in the region of interest (ROI) and the background noise.[22] The CNR is defined as:

$$\mathrm{CNR_m} = 10\log\left(\frac{\mu_m - \mu_b}{\sqrt{\sigma_m^2 + \sigma_b^2}}\right) \quad (1)$$

where μ_m and σ_m^2 indicate the mean and variance (of the gray values) of a $\mathrm{ROI_m}$ and μ_b, σ_b^2 are the mean and variance of the background area in the noisy image, respectively.

To compute the CNR for an image, at least two ROIs should be selected from the image. One of the regions represents a texture-free area from the background of the image ($\mathrm{ROI_1}$ in Figure 2f) and the other represents the ROI that contains the desired feature. In the current study, two sets of regions were considered as the desired areas. The first set of regions included the textural and edge areas of the lesion surface layer at the air–enamel boundary ($\mathrm{ROI_2}$) and the dentin–enamel junction ($\mathrm{ROI_3}$). The CNR index for these regions was shown as $\mathrm{CNR_{Edge}}$. The second set of regions included texture-free areas of the enamel ($\mathrm{ROI_4}$) and the dentin ($\mathrm{ROI_5}$) for which the index was shown as $\mathrm{CNR_{Tex\text{-}free}}$ (Figure 2f). The final CNR value for each set of regions was calculated by averaging the CNR values of different ROIs.

Edge preserving

The edge preserving index (EPI) evaluates the effect of noise reduction on the degradation of the image edges and measures the edge similarity between the original and denoised images over the locally selected ROI. EPI is defined as:

$$\mathrm{EPI_m} = \frac{\Gamma\left(\Delta I_m' - \Delta\bar{I}_m', \Delta I_m - \Delta\bar{I}_m\right)}{\sqrt{\Gamma\left(\Delta I_m' - \Delta\bar{I}_m', \Delta I_m' - \Delta\bar{I}_m'\right)\Gamma\left(\Delta I_m - \Delta\bar{I}_m, \Delta I_m - \Delta\bar{I}_m\right)}} \quad (2)$$

where I_m' and I_m are the intensities of the $\mathrm{ROI_m}$ containing edge information in noisy and denoised images, respectively. Δ is the Laplacian operator with a standard 3×3 window. $\bar{I}$ indicates the mean of I, and Γ is the correlation operator in the $\mathrm{ROI_m}$.[23]

In the current study, the ROI included two edge regions, the air–enamel and dentin–enamel boundaries ($\mathrm{ROI_2}$ and $\mathrm{ROI_3}$ in Figure 2f).

Blurring index

The blurring index (BI) evaluates the overall quality of the image. In image denoising, there is always a trade-off between increasing the smoothness and losing the fine details of the original image. Accordingly, an increase in the CNR value does not necessarily reflect the high performance of the denoising method as the blurring of the fine features can also lead to an increased CNR value. Other indexes such as the blurring index were therefore introduced to provide better justification regarding CNR values.[24] The blurring index is defined as:

$$\mathrm{Blurring} = \frac{T_H}{M \times N} \quad (3)$$

where T_H is the number frequency component of pixels with image intensity greater than $Fmax/1000$, F_{max} is the maximum absolute value of the frequency component, and $M \times N$ is the dimension of an image.

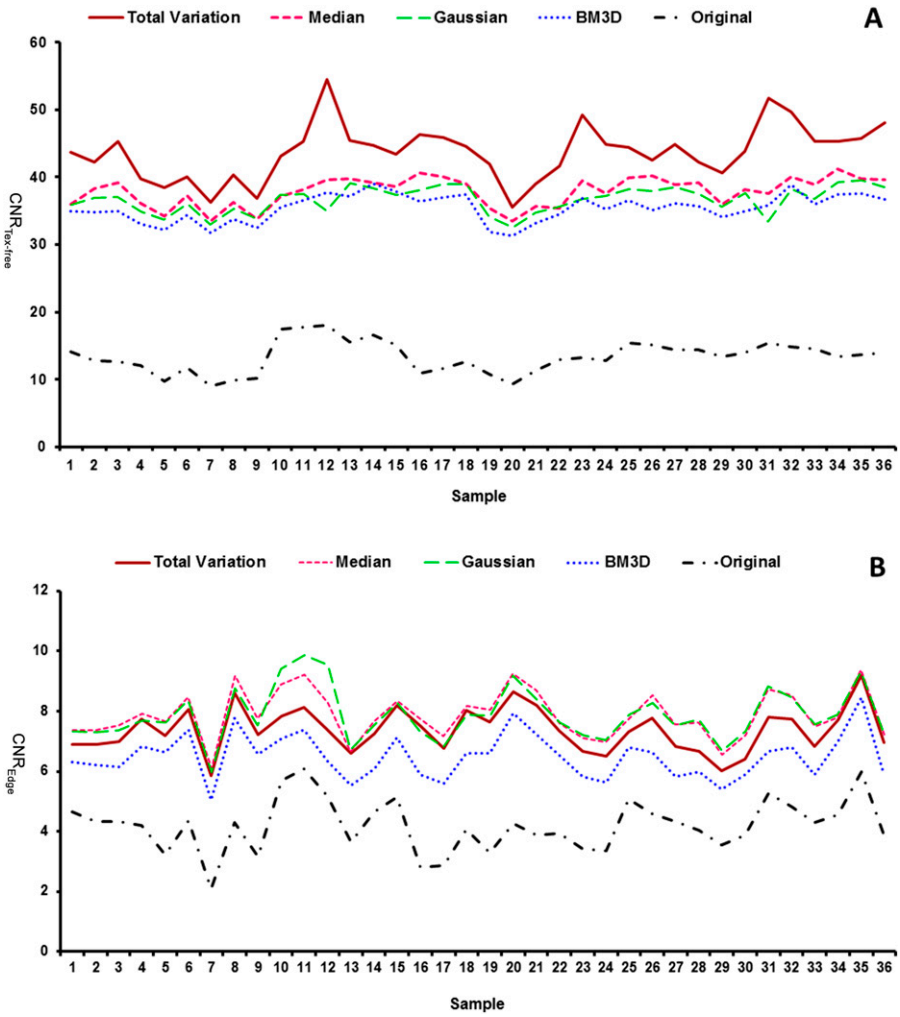

Figure 3 (a) Contrast-to-noise ratio (CNR) value in the texture-free area ($CNR_{Tex\text{-}free}$) of 36 specimens before and after denoising using the four methods; (b) CNR value in the edge and textural area (CNR_{Edge}) of 36 specimens before and after denoising using the four methods.

Qualitative analysis and visual evaluation by experts

Two experienced clinicians visually assessed and rated the diagnosability of the images before and after the denoising process. The visual evaluation was performed with the double-stimulus continuous quality scale procedure based on the recommendations of the International Telecommunication Union Radiocommunication Sector.[25]

A total of 470 images from 16 teeth with a range of features such as sound and carious enamel and dentin, hypomineralized enamel, cracked tooth and artificial caries were evaluated. The images included 47 original images of sound enamel and dentine, 47 original images of carious and lesion containing teeth and 376 denoised images by the 4 methods.

For each case, the clinicians were presented with the original and the denoised images randomly without labelling and were asked to allocate a score in the one-to-five scale. Score of one corresponded to the lowest and five to the highest subjective visual perception. The maximum score for each filter was 235, if the expert assigned the score of 5 for all 47 images denoised with a method. For each filter, the average score was computed and the score was divided by 2.35 to be expressed in percentage format.

In order to improve the visualization of the original and denoised images and to facilitate the visual perception of the filtering effect, the images were also colourized using the *colormapeditor* command by choosing Jet colormap in MATLAB. Fixed red, green and blue index values were set for all the colourized images.

Results

Figure 2a–e shows a sample original micro-CT image of a tooth with a natural enamel lesion along with the results of different denoising methods. The original image had a high level of noise content in the form of black and white dots which was also reflected in the colourized image.

Table 1 Average and standard deviation value of contrast-to-noise ratios (CNRs) in the texture-free area, CNRs in the edge area, EPI, blurring index, the performance time and the visual analysis score for the different denoising methods

Performance metric	*BM3D*	*Gaussian*	*Median*	*TV*	*Original*
$CNR_{Tex\text{-}free}$	35.40 ± 2.02	36.63 ± 1.93	37.85 ± 2.16	43.7 ± 4.06	13.35 ± 2.35
CNR_{Edge}	6.48 ± 0.75	7.73 ± 0.87	7.87 ± 0.79	7.37 ± 0.74	4.19 ± 0.88
EPI	0.51 ± 0.10	0.48 ± 0.09	0.50 ± 0.10	0.52 ± 0.10	1
Blurring index	0.0104 ± 0.0039	0.0026 ± 4.04	0.0055 ± 0.0029	0.0088 ± 0.0037	NA
Performance time	301.57 ± 12.88	0.0997 ± 0.075	49.72 ± 0.71	17.76 ± 0.97	NA
Visual analysis score (%)					
Lesion-containing teeth	94.82	35.95	25.31	69.21	81.05
Sound teeth images	89.54	35	34.80	100	75.60
Overall average	92.18	35.47	30.05	84.60	78.32

BM3D, block-matching and three-dimensional; CNR_{Edge}, CNR value in the edge area; $CNR_{Tex\text{-}free}$, CNR value in the texture-free area; EPI, edge preserving index; NA, not available; TV, total variation.

In addition, the original image suffered from the presence of ring artefact which resembles concentric rings in the dentin area. The feature of interest in this specimen was an enamel lesion. The lesion had the classic triangular shape with a wide base towards the external surface of the tooth and two advancing front tips towards the dentin–enamel junction. There was a high mineral density layer with an average thickness of 30 μm at the surface of the lesion.

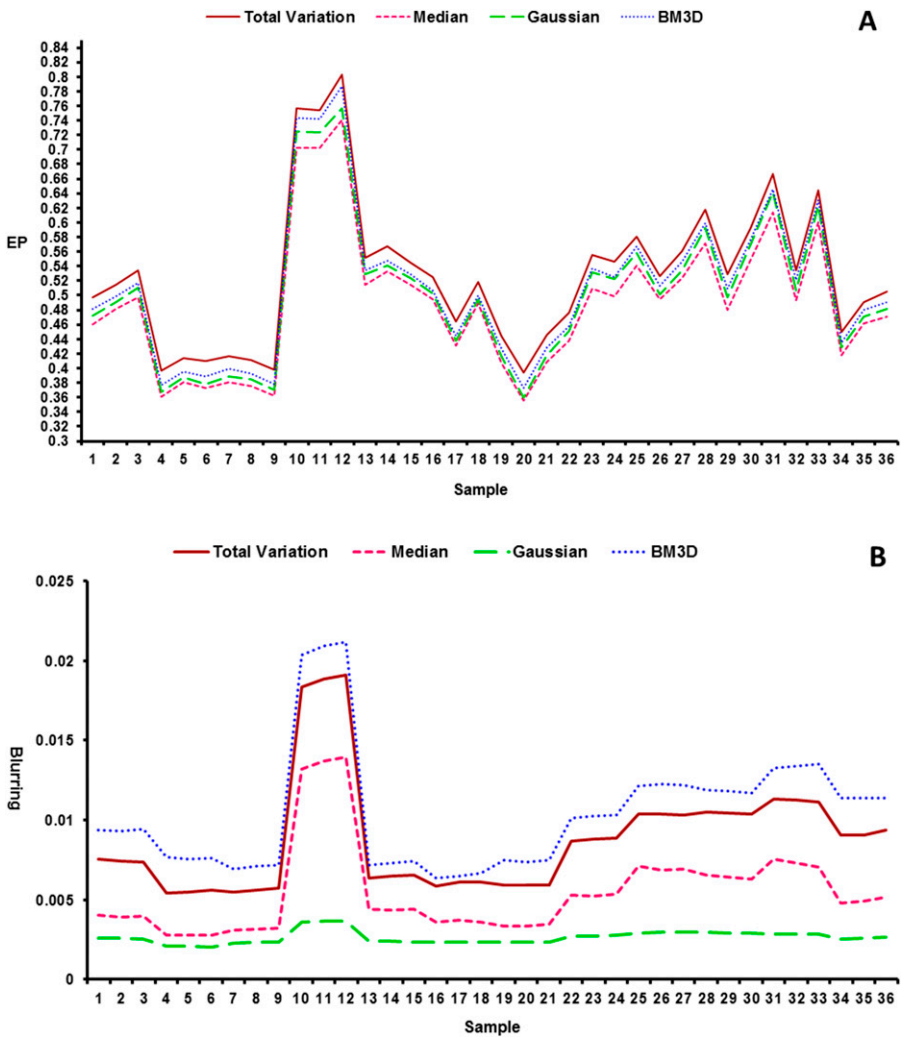

Figure 4 (a) Edge preserving index value for 36 image specimens after denoising using the four methods. (b) Blurring index value for 36 image specimens after denoising using the four methods.

Quantitative analysis of denoising methods
The quantitative analysis was performed on 180 micro-CT images (including 36 original and 144 denoised images using 4 methods), and the values of 3 indexes were calculated for each image.

Contrast-to-noise ratio
Figure 3a,b shows the CNR values of the original and denoised micro-CT images in the texture-free and edge areas, respectively.

For all the specimens, the denoising process led to an increase in the CNR value in both the texture-free and edge areas. However, this increase was more significant in the texture-free area than in the edge and textural area. Accordingly, following the noise-reduction process, the average CNR value at the texture-free area in all specimens (Table 1) increased from 13.35 ± 2.35 in the original images to 35.40 ± 2.02 (+62.28%) in images denoised using the BM3D method, to 36.63 ± 1.93 (+63.5%) in images denoised using the gaussian method, to 37.85 ± 2.16 (+64.72%) in images denoised using the median method and to 43.7 ± 4.06 (+69.45%) in images denoised using the total variation method.

In the texture-free area, the highest $CNR_{Tex\text{-}free}$ value was achieved by the total variation method followed by the median, gaussian and BM3D methods, respectively. However, in the textural and edge areas, the highest CNR_{Edge} value was achieved using the median and gaussian filters followed by the total variation and BM3D methods, respectively. It should be noted that despite the non-textural areas where higher CNR values indicate more smoothening and therefore are more desirable, in the textural and edge areas, lower CNR values which show sharper edges and less texture smoothing are preferred. The great challenge with all denoising methods is the loss of information and sharpness in the textural areas compared with the original image. Accordingly, our goal was to obtain lower values of $CNR_{\_Edge}$ as close to the original image as possible. Therefore, the most favourable smoothening performance in the textural and edge area was obtained by the BM3D method and in the non-textural areas by the total variation method. These results indicate that while total variation had the best performance in smoothing the non-textural areas of the images, the BM3D had the least degrading effect on the fine textural features of the images such as thin surface layer of the artificial lesions.

Edge preserving
The EP index is normalized in the [0 1] interval, for which higher values closer to 1 indicate better edge preservation and greater similarity. The results (Figure 4a) indicated that the highest edge-preserving value was achieved using the total variation method followed by the BM3D, gaussian and median denoising methods, respectively. The mean and standard deviation of the EP index for all images denoised using each of the methods are presented in Table 1.

Blurring index
The results of the blurring index analysis indicated that the BM3D method produced the highest blurring index value followed by the total variation, median and gaussian methods, respectively (Figure 4b). Based on the definition of the blurring index, the higher blurring index value indicates less blurring and sharper image. Accordingly, the BM3D method caused the least blurring and the gaussian method caused the highest blurring of the images. The severe blurring effect of the gaussian method can be observed from the colourized image where the colour change at the enamel–air boundary and dentin–enamel junction happens gradually owing to blurring and loss of sharpness at the edges (Figure 2b,d).

Qualitative analysis and visual evaluation
The results of the visual analysis indicated that for images with very fine features of interest such as the thin surface layer of the carious enamel lesion and small enamel caries, clinicians gave the highest score to BM3D denoised images (94.82%) followed by the original image (81.05%), and the total variation (69.21%), the gaussian (35.95%) and the median (25.31%) denoised images. For images of sound teeth without very fine features, the clinicians gave the highest score to total variation (100%) followed by BM3D (89.54%), original (75.60%), gaussian (35%) and median (34.80%) denoised images.

In addition to removing the noise content and preserving the diagnostic information, the effect of the denoising methods on eliminating the ring artefact in the images was also considered in the visual evaluation by the clinicians. As seen in Figures 2c and 3c, the total variation method had the best performance in eliminating ring artefacts followed by the gaussian, median and BM3D methods.

Based on the overall results of the visual evaluation of sound and non-sound dental images, the BM3D method gained the highest score followed by the total variation, original, gaussian and median methods, respectively.

Performance time
The performance time is a critical parameter in image-processing methods, as it considers the required time for implementing an algorithm on a defined number of images. In micro-CT imaging, each scan of a single specimen produces a large number of images (>1000 images for scanning a premolar crown with an image resolution of 8.9 μm) and therefore the performance time of denoising and analysis processes is of great significance.

Evaluation of the time penalty of various methods for denoising a stack of dental micro-CT images on a personal computer with Microsoft® Windows X32 edition (Microsoft Corporation, Seattle, WA), Intel® Core™ i7 central processing unit (Q740 @1.73 GHz) and 4.00-GB random-access memory (Intel Corporation), showed that the longest execution time occurred with the BM3D method (301.57 ± 12.88 s), which was considerably higher than for the other methods including the median (49.72 ± 0.71 s), total variation (17.76 ± 0.97 s) and gaussian methods (0.0997 ± 0.075 s), respectively.

Discussion

The major dilemma in all denoising methods is filtering out the noise content as much as possible while preserving the important features of the original image such as texture, contour and fine details. To address these two conflicting issues, we applied two advanced denoising algorithms and used three image analysis parameters to evaluate the smoothness (CNR), edge preservation and blurring of denoised images in relation to the original image. Each of these indexes assesses a different specific aspect of the denoising performance, and therefore all of them should be considered together before making a comprehensive judgment. In addition, a subjective visual assessment of the images was performed to appreciate the practical performance of the denoising methods from the clinicians' point of view. To our knowledge, very few studies[26,27] have investigated the denoising of dental radiographs, and in fact, the current study is the first to propose and evaluate the application of the BM3D and total variation methods for denoising dental micro-CT images.

Based on the outcomes of the quantitative and qualitative evaluation of the denoising methods, the BM3D method exhibited the best performance by having the highest level of preservation of the textural features (CNR_{Edge}), the lowest blurring of the whole image (BI), the highest clinical visual score in images with very fine features and the highest overall visual score for all types of images. The BM3D method also had the second best value of the EP index among the other denoising methods which shows a high level of edge preservation in denoised images.

Despite the high performance and great advantages of the BM3D method, it could not completely remove ring artefacts from the original images and the smoothing of the texture-free area was the lowest compared with the other methods. In addition, the high time penalty of this method was a disadvantage compared with the other denoising methods which were significantly faster. Yet, the clinicians preferred the BM3D method in the subjective visual analysis, as it could remove the greatest amount of noise content while still preserving the small and thin textural features such as cracks and the surface layer of enamel caries. In fact, the BM3D method had the best trade-off between smoothening of the texture-free areas and preservation of information in the textural areas with the lowest level of blurring.

On the other hand, the total variation method provided the best results with regard to smoothing of the image in texture-free areas and preserving the edges and borders of the image features. These issues were reflected by the value of $CNR_{Tex\text{-}free}$ and EP indexes, which were the highest for the total variation method among the other methods. These results were also confirmed by the subjective visual evaluation of the sound teeth images in which the total variation method obtained a 100% visual score by both the clinicians. The visual comparison of the total-variation denoised images with TMR images, as the smoothness model, indicated outright similarity with the TMR images and excellent removal of noise in micro-CT images.

TMR is considered as the gold standard two-dimensional technique for the evaluation of carious lesions,[28] which produces high-quality images with minimal noise owing to the micron-range thickness of the specimens. However, it has limitations such as the need for destructive sectioning of the specimen and the impossibility for 3D studies. Although previous studies have found good correlation between micro-CT and TMR results,[29] TMR produces smoother images with greater details owing to the higher noise content in micro-CT images.[28]

In the current study, we could achieve very-low-noise micro-CT images with similar quality to TMR images using the total variation method. These images obtained 100% visual score in sound teeth, and the clinicians confirmed excellent denoising and similarity with TMR. However, considering the non-preservation of very fine textural features, revealed by subjective evaluation of images with small lesions, there is a need for optimization of the total variation method, which can be a topic for future research.

The other significant finding of this study was the high capacity of the total variation method in eliminating ring artefacts, which minimizes the need for repeating the entire imaging procedure or extra processing[30] for ring artefact removal. This feature of the total variation method relates to its high smoothing performance, which is reflected by the high value of the $CNR_{Tex\text{-}free}$ for this method.

Regarding the performance time, although the total variation method had a higher time penalty than the gaussian and median methods, it was however significantly faster than the BM3D method and thus may still be considered as a fast denoising approach.

The two classic denoising methods of gaussian and median, which have been commonly applied for denoising dental micro-CT images, had very low performance regarding the preservation of the edges and caused significant blurring of the denoised images. Similarly, clinicians gave the lowest scores to

these two methods regarding their clinical diagnostic value. In fact, these methods obtained lower scores than the original image when implemented at their full capacity.

In general, each denoising approach has its assumptions, advantages and limitations, and the selection of each method depends on the type of image, noise model and application purpose.[31] However, considering the findings of this study, we may suggest the BM3D method as the most reliable and accurate technique for denoising images with very fine details, such as shallow artificial and natural enamel lesions, as well as other fine biological and artificial structures in which the preservation of the texture and fine features of the image is of the greatest importance. On the other hand, the total variation method is the technique of choice for denoising images without very small details or fine textures in which the clinician or researcher is interested, mainly for anatomical features and structural measurements of the dental tissue. In addition, it is the best technique for denoising micro-CT images that require removal of ring artefacts.

In terms of possible improvements and future research, we suggest that the focus be on improving the performance of the total variation and BM3D methods, as their contribution in enhancing the quality of micro-CT images may make micro-CT a reliable substitute for TMR in all cases.

Finally, the promising results obtained by the two new denoising methods provide an impetus for future research into the issue of noise elimination and quality enhancement for other types of dental images, including CBCT, periapical and panoramic radiography.

Acknowledgments

The first author thanks Dr Peter Duc Hoang, Dr Neha Pandey, Colgate Australia and the Australian Center for Microscopy and Microanalysis (ACMM).

References

1. Zou W, Hunter N, Swain MV. Application of polychromatic μCT for mineral density determination. *J Dent Res* 2011; **90**: 18–30. doi: 10.1177/0022034510378429
2. Swain MV, Xue J. State of the art of Micro-CT applications in dental research. *Int J Oral Sci* 2009; **1**: 177–88. doi: 10.4248/IJOS09031
3. Chappard C, Basillais A, Benhamou L, Bonassie A, Brunet-Imbault B, Bonnet N, et al. Comparison of synchrotron radiation and conventional X-ray microcomputed tomography for assessing trabecular bone microarchitecture of human femoral heads. *Med Phys* 2006; **33**: 3568–77. doi: 10.1118/1.2256069
4. Boas FE, Fleischmann D. CT artifacts: causes and reduction techniques. *Imaging Med* 2012; **4**: 229–40. doi: 10.2217/iim.12.13
5. Taylor AM, Satterthwaite JD, Ellwood RP, Pretty IA. An automated assessment algorithm for micro-CT images of occlusal caries. *Surgeon* 2010; **8**: 334–40. doi: 10.1016/j.surge.2010.06.007
6. Buades A, Coll B, Morel JM. On image denoising methods. *CMLA Preprint* 2004; **5**.
7. Buades A, Coll B, Morel JM. A review of image denoising algorithms, with a new one. *Multiscale Model Simul* 2005; **4**: 490–530. doi: 10.1137/040616024
8. Rebaudi A, Koller B, Laib A, Trisi P. Microcomputed tomographic analysis of the peri-implant bone. *Int J Periodontics Restorative Dent* 2004; **24**: 316–25.
9. Nevins ML, Camelo M, Rebaudi A, Lynch SE, Nevins M. Three-dimensional micro-computed tomographic evaluation of periodontal regeneration: a human report of intrabony defects treated with Bio-Oss collagen. *Int J Periodontics Restorative Dent* 2005; **25**: 365–73.
10. Huang TT, Jones AS, He LH, Darendeliler MA, Swain MV. Characterisation of enamel white spot lesions using X-ray microtomography. *J Dent* 2007; **35**: 737–43. doi: 10.1016/j.jdent.2007.06.001
11. Huang TT, He LH, Darendeliler MA, Swain MV. Correlation of mineral density and elastic modulus of natural enamel white spot lesions using X-ray microtomography and nanoindentation. *Acta Biomater* 2010; **6**: 4553–9. doi: 10.1016/j.actbio.2010.06.028
12. Nakata K, Nikaido T, Nakashima S, Nango N, Tagami J. An approach to normalizing micro-CT depth profiles of mineral density for monitoring enamel remineralization progress. *Dent Mater J* 2012; **31**: 533–40. doi: 10.4012/dmj.2011-228
13. Neves Ade A, Coutinho E, Vivan Cardoso M, Jaecques SV, Van Meerbeek B. Micro-CT based quantitative evaluation of caries excavation. *Dental Mater* 2010; **26**: 579–88. doi: 10.1016/j.dental.2010.01.012
14. De Vos W, Casselman J, Swennen GR. Cone-beam computerized tomography (CBCT) imaging of the oral and maxillofacial region: a systematic review of the literature. *Int J Oral Maxillofac Surg* 2009; **38**: 609–25. doi: 10.1016/j.ijom.2009.02.028
15. De Medeiros RC, Soares JD, De Sousa FB. Natural enamel caries in polarized light microscopy: differences in histopathological features derived from a qualititative approach to interpret enamel birefringence. *J Microscopy* 2012; **246**: 177–89.
16. Shahmoradi M, Bertassoni LE, Elfallah HM, Swain M. Fundamental structure and properties of enamel, dentin and cementum. In: Ben-Nissan, ed. *Advances in calcium phosphate biomaterials*. Heidelberg, Germany: Springer; 2014. pp. 511–47.
17. Danielyan A, Katkovnik V, Egiazarian K. BM3D frames and variational image deblurring. *IEEE Trans Image Process* 2012; **21**: 1715–28. doi: 10.1109/TIP.2011.2176954
18. Dabov K, Foi A, Katkovnik V, Egiazarian K. Image denoising by sparse 3-D transform-domain collaborative filtering. *IEEE Trans Image Process* 2007; **16**: 2080–95. doi: 10.1109/TIP.2007.901238
19. Strong D, Chan T. Edge-preserving and scale-dependent properties of total variation regularization. *Inverse Probl* 2003; **19**: S165. doi: 10.1088/0266-5611/19/6/059
20. Burger W, Burge MJ. Digital image processing: an algorithmic introduction using Java. New York, NY: Spinger-Verlag; 2009.
21. Rudin LI, Osher S, Fatemi E. Nonlinear total variation based noise removal algorithms. *Physica D* 1992; **60**: 259–68. doi: 10.1016/0167-2789(92)90242-F
22. Kafieh R, Rabbani H, Selesnick I. Three dimensional data-driven multi scale atomic representation of optical coherence tomography. *IEEE Trans Med Imaging* 2015; **34**: 1042–62. doi: 10.1109/TMI.2014.2374354
23. Sattar F, Floreby L, Salomonsson G, Lovstrom B. Image enhancement based on a nonlinear multiscale method. *IEEE Trans Image Process* 1997; **6**: 888–95. doi: 10.1109/83.585239

24. De K, Masilamani V. Image sharpness measure for blurred images in frequency domain. *Proced Eng* 2013; **64**: 149–58. doi: 10.1016/j.proeng.2013.09.086
25. Loizou CP, Pattichis CS, Christodoulou CL, Istepanian RS, Pantziaris M, Nicolaides A. Comparative evaluation of despeckle filtering in ultrasound imaging of the carotid artery. *IEEE Trans Ultrason Ferroelectr Freq Control* 2005; **52**: 1653–69. doi: 10.1109/TUFFC.2005.1561621
26. Serafini T, Zanella R, Zanni L. Gradient projection methods for image deblurring and denoising on graphics processors. In: Chapman B, ed. *Parallel computing: from multicores and GPU's to petascale*. Amsterdam, Netherlands: IOS Press BV; 2010.
27. Frosio I, Olivieri C, Lucchese M, Borghese NA, Boccacci P. Bayesian denoising in digital radiography: a comparison in the dental field. *Comput Med Imaging Graph* 2013; **37**: 28–39. doi: 10.1016/j.compmedimag.2012.10.003
28. Hamba H, Nikaido T, Sadr A, Nakashima S, Tagami J. Enamel lesion parameter correlations between polychromatic micro-CT and TMR. *J Dent Res* 2012; **91**: 586–91. doi: 10.1177/0022034512444127
29. Lo E, Zhi QH, Itthagarun A. Comparing two quantitative methods for studying remineralization of artificial caries. *J Dent* 2010; **38**: 352–9. doi: 10.1016/j.jdent.2010.01.001
30. Sijbers J, Postnov A. Reduction of ring artefacts in high resolution micro-CT reconstructions. *Phys Med Biol* 2004; **49**: N247–53. doi: 10.1088/0031-9155/49/14/N06
31. Kaur J, Kaur M, Kaur P, Kaur M. Comparative analysis of image denoising techniques. *Int J Emerg Technol Adv Eng* 2012; **2**: 296–8.